Static tool influence function for fabrication simulation of hexagonal mirror segments for extremely large telescopes

Dae Wook Kim and Sug-Whan Kim

Space Optics Laboratory, Department of Astronomy, Yonsei University, Seoul, Republic of Korea
Institute of Space Science and Technology, Yonsei University, Seoul, Republic of Korea
Center for Space Astrophysics, Yonsei University, Seoul, Republic of Korea
letter2dwk@hotmail.com, skim@galaxy.yonsei.ac.kr

Abstract: We present a novel simulation technique that offers efficient mass fabrication strategies for 2m class hexagonal mirror segments of extremely large telescopes. As the first of two studies in series, we establish the theoretical basis of the tool influence function (TIF) for precessing tool polishing simulation for non-rotating workpieces. These theoretical TIFs were then used to confirm the reproducibility of the material removal foot-prints (measured TIFs) of the bulged precessing tooling reported elsewhere. This is followed by the reverse-computation technique that traces, employing the simplex search method, the real polishing pressure from the empirical TIF. The technical details, together with the results and implications described here, provide the theoretical tool for material removal essential to the successful polishing simulation which will be reported in the second study.

OCIS codes: (220.0220) Optics design and fabrication; (220.1250) Aspherics; (220.4610) Optics fabrication; (220.5450) Polishing

References and links

1. T. Andersen, A. L. Ardeberg, J. Beckers, A. Goncharov, M. Owner-Petersen, H. Riewaldt, R. Snel, and D. D. Walker, "The Euro50 Extremely Large Telescope," in *Future Giant Telescopes*, J. R. P. Angel and R. Gilmozzi, eds., Proc. SPIE **4840**, 214-225 (2003).
2. D. D. Walker, A. P. Doel, R. G. Bingham, D. Brooks, A. M. King, G. Peggs, B. Hughes, S. Oldfield, C. Dorn, H. McAndrews, G. Dando, and D. Riley, "Design Study Report: The Primary and Secondary Mirrors for the Proposed Euro50 Telescope" (2002), http://www.zeeko.co.uk/papers/dl/New%20Study%20Report%20V%2026.pdf.
3. T. Anderson, A. Ardeberg, and M. Owner-Perterson, "EURO50: Design study of a 50m adaptive optics telescope" (2003), http://www.astro.lu.se/~torben/euro50/publications/white_book80.pdf.
4. P. Dierickx, "Optical fabrication in the large," in *Proceedings of the Backaskog workshop on extremely large telescopes*, T. Andersen, A. Ardeberg, and R. Gilmozzi, eds., no. 57 of ESO conference and workshop proceedings (Lund Observatory and European Southern Observatory, Munchen, 2000), pp. 224-236.
5. H. M. Martin, D. S. Anderson, J. R. P. Angel, R. H. Nagel, S. C. West, and R. S. Young, "Progress in the stressed-lap polishing of a 1.8-m f/1 mirror," in *Advanced Technology Optical Telescopes IV*, L. D. Barr, Ed., Proc. SPIE **1236**, 682-690 (1990).
6. A. R. Jones and J. W. Rupp, "Rapid optical fabrication with computer-controlled optical surfacing," Opt. Eng. **30**, 1962-1967 (1991).
7. T. S. Mast and J. E. Nelson, "Fabrication of large optical surfaces using a combination of polishing and mirror bending," in *Advanced Technology Optical Telescopes IV*, L. D. Barr, Ed., Proc. SPIE **1236**, 670-681 (1990).
8. L. N. Allen, "Progress in ion figuring large optics," in *Laser-Induced Damage in Optical Materials*, H. E. Bennett, A. H. Guenther, M. R. Kozlowski, B. E. Newnam, and M. J. Soileau, Eds., Proc. SPIE **2428**, 237-247 (1995).
9. F. A. Carbone and D. A. Markle, "Combining ion figuring and SPSI testing to produce a high-quality aspheric 18-inch-diameter f/2 mirror," in *Optical Manufacturing and Testing*, V. J. Doherty D. V. M. and H. P. Stahl, Eds., Proc. SPIE **2536**, 89-98 (1995).
10. K. Beckstette, M. Küchel, and E. Heynacher, "Large mirror figuring and testing," Astrophys Space Sci. **160**, 207-214 (1989).

#6258 - $15.00 US Received 10 January 2005; revised 27 January 2005; accepted 27 January 2005

11. T. K. Korhonen and T. Lappalainen, "Computer-controlled figuring and testing," in *Advanced Technology Optical Telescopes IV*, L. D. Barr, Ed., Proc. SPIE **1236**, 691-694 (1990).
12. T. S. Mast, J. E. Nelson, and G. E. Sommargren, "Primary mirror segment fabrication for CELT," in *Optical Design, Materials, Fabrication, and Maintenance*, P. Dierickx, ed., Proc. SPIE **4003**, 43-58 (2000).
13. D. D. Walker, A. T. Beaucamp, R. G. Bingham, D. Brooks, R. Freeman, S. W. Kim, A. King, G. McCavana, R. Morton, D. Riley, and J. Simms, "Precessions aspheric polishing : - new results from the development programme," in *Optical Manufacturing and Testing V*, H. P. Stahl, ed., Proc. SPIE **5180**, 15-28 (2004).
14. D. D. Walker, D. Brooks, A. King, R. Freeman, R. Morton, G. McCavana, and S. W. Kim, "The 'Precessions' tooling for polishing and figuring flat, spherical and aspheric surfaces", Opt. Express, **11**, 958-964 (2003).
15. D. D. Walker, A. T. Beaucamp, D. Brooks, V. Doubrovski, M. D. Cassie, C. Dunn, R. R. Freeman, A. King, M. Libert, G. McCavana, R. Morton, D. Riley, and J. Simms, "New results from the Precessions polishing process scaled to larger sizes," in *Optical Fabrication, Metrology, and Material Advancements for Telescopes*, E. Atad-Ettedgui and P. Dierickx, eds., Proc. SPIE **5494**, 71-80 (2004).
16. D. D. Walker, A. T. Beaucamp, D. Brooks, V. Doubrovski, M. D. Cassie, C. Dunn, R. R. Freeman, A. King, M. Libert, G. McCavana, R. Morton, D. Riley, and J. Simms, "Recent developments of Precessions polishing for larger components and free-form surfaces," in *Current Developments in Lens Design and Optical Engineering V*, P. Z. Mouroulis, W. J. Smith, and R. B. Johnson, eds., Proc. SPIE **5523**, 281-289 (2004).
17. D. W. Kim, Space Optics Laboratory, Yonsei University, 134 Shinchon-dong, Sudaemun-gu, Seoul, Republic of Korea and S. W. Kim are preparing a manuscript to be called "Novel polishing algorithm for fabrication simulation of 2m class hexagonal mirror segments for extremely large telescopes."
18. H. Lee, Space Optics Laboratory, Yonsei University, 134 Shinchon-dong, Sudaemun-gu, Seoul, Republic of Korea and S. W. Kim are preparing a manuscript to be called "Non-linear variation of tool influence function in precessing sub-diameter tool polishing."
19. J. C. Lagarias, J. A. Reeds, M. H. Wright, and P. E. Wright, "Convergence Properties of the Nelder-Mead Simplex Method in Low Dimensions," SIAM Journal of Optimization, **9**, 112-147 (1998).

1. Introduction

The Extremely Large Telescopes (ELTs), currently being planned, are to have hexagonal segmented primary mirrors of about 1-2m in diameter [1]. The target specifications of these ELT primary mirrors are highly challenging. Examples may include the EURO50 primary mirror system consisted of 618 hexagonal segments. Each segment is to have the surface form accuracy of better than 18nm peak-to-valley [2]. The primary mirror system is to be phased and aligned to the precision of about 10-20nm rms [3]. The continuing change in slope difference between the target shape and the best-fit sphere serves as the primary cause to the fabrication difficulty. This is expressed as fabrication difficulty index *dy* [4] in Table 1. Mathematically, *dy* is defined as

$$dy = \frac{8(f/D)^3}{k}, \tag{1}$$

where k is the conic constant of the primary mirror, f the focal length, and D the diameter of the primary mirror. The table shows that, even without considering mass fabrication requirement, the EURO50 primary segment (dy=4.92) is about 5.3 times more difficult than the KECK primary segment (dy=26.1).

In the midst of many fabrication technologies developed over the last few decades [5-11], the ion beam figuring technique [8,9] has demonstrated success at producing large hexagonal mirror of about 15nm rms [4]. However, the technique has extremely low material removal rates and consequently suffers from the long delivery schedule. A study indicated that using 6 ion figuring chambers would take about 8 years to complete the 1080 0.5m diameter segments for CELT [12]. This does not even include the requirement of a number of the precision grinding and pre-polishing machines for producing the input mirror surfaces, of sub-micron accuracy, to the ion figuring machines. This demonstrates the critical limitation of its general applicability to the mass fabrication requirement for ELT primary mirror segments of up to 2m in diameter, within the reasonable delivery time of 2-3 years.

#6258 - $15.00 US Received 10 January 2005; revised 27 January 2005; accepted 27 January 2005

Table 1. Specifications of three ELTs and KECK primary mirrors

Telescope	Primary Mirror Diameter (m)	Primary Mirror f-ratio	Segment Size (m)	Conic Constant	No. of Segments	*dy*	Segment Shape
EURO50	50.4	f/0.85	2	-0.9994	618	4.92	Hexagonal
OWL	100	f/1.82 or f/1.5	1.6	0	3048	n/a	Hexagonal
CELT	30	f/1.50	0.5	-1.525	1080	17.7	Hexagonal
KECK	10	f/1.75	1.8	-1.644	36	26.1	Hexagonal

Among the many process elements, three are crucial for the successful deployment of efficient mass fabrication technique for ELT segmented mirrors. They are: i) low tooling overhead, ii) deterministic material removal and iii) embedded process control intelligence. The bulged precessing polishing process [13,14], recently introduced, may have potentials to bring greater improvement than earlier methods [5-11] for the three elements defined above. In particular, as it moves across the workpiece, the bulged precessing tool tends to conform its shape to the local surface. Additionally, by changing the tool pressure, a wide range of surface contact area is achieved between the tool and the workpiece using a single bonnet. Such flexible tooling ability, aided with a precision 7-axis (including workpiece rotation) CNC capability and the built-in process intelligence, demonstrated the p-v form accuracy of about 1μm for an on-axis ellipsoid of 500mm in diameter [15,16].

This process, as is of today, exhibits its limitation to immediate applicability for the fabrication of ELT primary mirror segments in terms of their size, the aforementioned target surface specification and the hexagonal shape. The production is further complicated with the mass fabrication requirement within the reasonable delivery schedule of 2-3 years. This gives rise to the need of an improved fabrication technique capable of processing the axially non-symmetric workpieces with even higher deterministic material removal controllability, added to the existing bulged precessing tooling.

Section 2 deals with the theoretical background of the static tool influence function (sTIF) for non-rotating workpieces and its experimental verification. This is followed by the reverse computation technique for the real polishing pressure exerted from the precessing tool bonnet system in Section 3. Section 4 summarizes the implications of this study in view of polishing simulation of hexagonal mirror segments for ELT. To this extent, the present technical development, reported here, lay the theoretical foundation for a new precession polishing simulation technique [17] that may offer an attractive solution to the challenging problems of mass fabrication of segmented mirrors for the ELT projects.

2. sTIF generation and verification

2.1. sTIF

For circularly symmetric rotating workpieces, the generalized equation of material removal (EMR) and the variable tool influence function (vTIF) are soon to be reported [18]. EMR is derived from the well-known Preston's relation expressed as

$$\Delta z = \kappa P V_T \Delta t, \tag{2}$$

where Δz is the integrated material removal from the workpiece surface, κ the removal coefficient of the segment material, P the polishing pressure, V_T the magnitude of relative speed between the tool and workpiece surface, and Δt the dwell time.

Earlier studies [13-16] showed that the precessing polishing process currently in service uses the measured TIFs of near Gaussian shapes to compute the required dwell time. That

#6258 - $15.00 US Received 10 January 2005; revised 27 January 2005; accepted 27 January 2005

method bypasses the need for prior knowledge of the relationship among the material removal (i.e., TIF), polishing pressure, and velocity inside the tool-workpiece contact area (polishing spot). Nevertheless, we note that the relationship serves as an invaluable aid to further the process development for the precessing tool polishing.

The very shape of measured TIFs supports speculation that the polishing pressure exerted by the bonnet system is likely to be near Gaussian. This view is further strengthened with the integrated velocity field that tends to be randomized by the tool precessing action over the dwell time. Thus, we take the approach, as depicted in Fig. 1(a), that the construction of theoretical TIF starts with a modified Gaussian function with standard deviation σ and maximum pressure P_T, such that

$$P = P_T(\exp(-\frac{\lambda^2}{2\sigma^2}))^{\psi}, \tag{3}$$

where λ is the distance between A and C, and ψ the modification coefficient. For non-rotating workpiece surfaces, the total relative speed V_T is the magnitude of the vector sum of the tool rotation $\overrightarrow{\mathbf{V_{TR}}}$ and the feed rate $\overrightarrow{\mathbf{V_{TF}}}$ shown in Fig. 1(b). This can be expressed as Eq. (4).

$$V_T = [(V_{TRx} + V_{TFx})^2 + (V_{TRy} + V_{TFy})^2]^{1/2} \tag{4}$$

Substituting Eq. (3) and (4) for P and V_T of Eq. (2), EMR for non-rotating workpieces is obtained as Eq. (5).

$$\Delta z = \kappa P_T(\exp(-\frac{\lambda^2}{2\sigma^2}))^{\psi}[(V_{TRx} + V_{TFx})^2 + (V_{TRy} + V_{TFy})^2]^{1/2}\Delta t \tag{5}$$

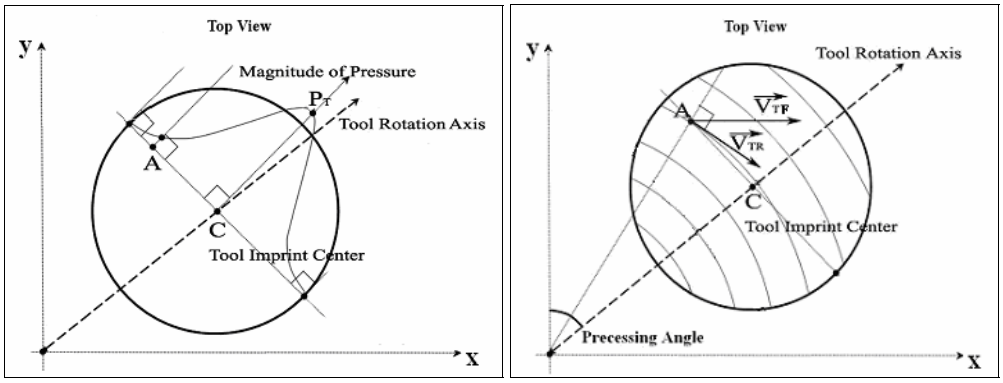

(a) (b)

Fig. 1. (a) Gaussian pressure distribution and (b) velocity components overlaid onto concentric speed contours of tool rotation inside the polishing spot (tool-workpiece contact area)

Eq. (5) can produce a wide variety of sTIF depending on the input polishing parameters, including tool rpm (W_T), inclination angle (α) and tool pressure (P_T). A typical example of sTIF is shown in Fig. 2. Here we note the shape difference between the two sTIF cross-sectional profiles shown in Fig. 2(b); this being caused by the asymmetric velocity field effect with the fixed precessing angle as depicted in Fig. 1(b). This result re-confirms the report that the asymmetric tool velocity field is strongly tied with changes in precessing angle [18]. For this reason, three precessing angles separated by 120 degrees were used to generate circularly symmetric sTIF throughout this study.

#6258 - $15.00 US Received 10 January 2005; revised 27 January 2005; accepted 27 January 2005

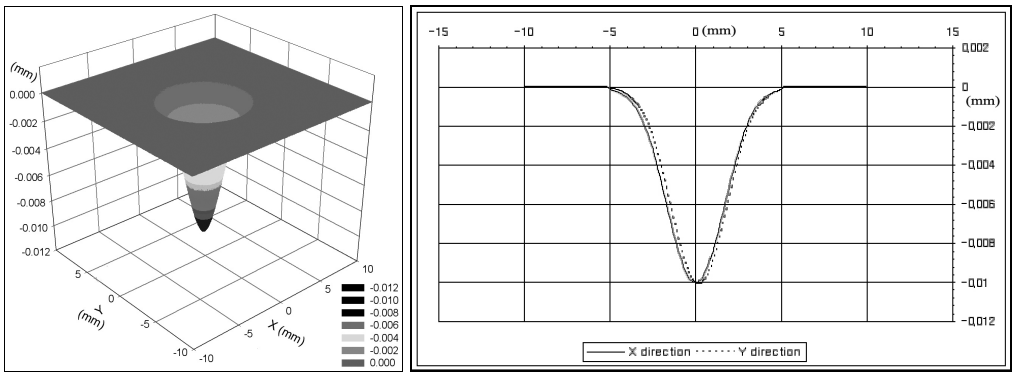

(a) (b)

Fig. 2. (a) Three dimensional view of sTIF and (b) cross-sectioned profiles of sTIF in X and Y axis (Δt=6 sec, W_T=1000 rpm, P_T=0.013 Mpa, α=15 degrees)

2.2. Experimental verification of sTIF

These theoretical TIFs were used to re-produce the characteristics of the measured [13,14] TIFs. First, Fig. 3 shows a family of 10 theoretical TIFs generated with the tool rotation range of 100-1000 rpm, with all other parameters fixed. It re-produced the measured material removal depth [14] versus the tool rotation. This implies that the material removal controllability can be achieved, both in simulation and in actual polishing, by altering the tool rotation.

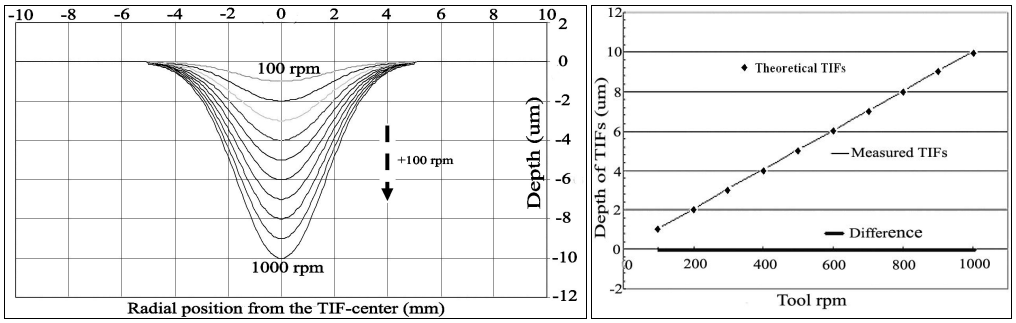

(a) (b)

Fig. 3. (a) Cross-sectional profiles of sTIFs (100 - 1000 tool rpm) and (b) depth of measured [14] and theoretical sTIFs

Second, we then tested the effects of workpiece attack (i.e. inclination) angle onto TIF as shown in Fig. 4. Whilst exhibiting the minor difference of about 30nm over the inclination range of 14-18 degrees, the overall diagram shows the theoretical TIFs following the measurement [13] very closely.

Third, we generated a family of theoretical TIFs with the tool pressure ranging from 0.0130 Mpa to 0.0214 Mpa, while holding the other control parameters fixed. The measured [14] and theoretical TIFs are presented in Fig. 5. Once again, the measured material removal depth and tool imprint radius were well reproduced with the theoretical TIFs. The minor difference in the cross-sectional profile width of both theoretical and experimental TIFs at $P_T \geq 0.0179$ Mpa can be corrected by either adjusting the parameters of the modified Gaussian function in Eq. (3), or altering the tool material (i.e. polishing cloth).

#6258 - $15.00 US Received 10 January 2005; revised 27 January 2005; accepted 27 January 2005

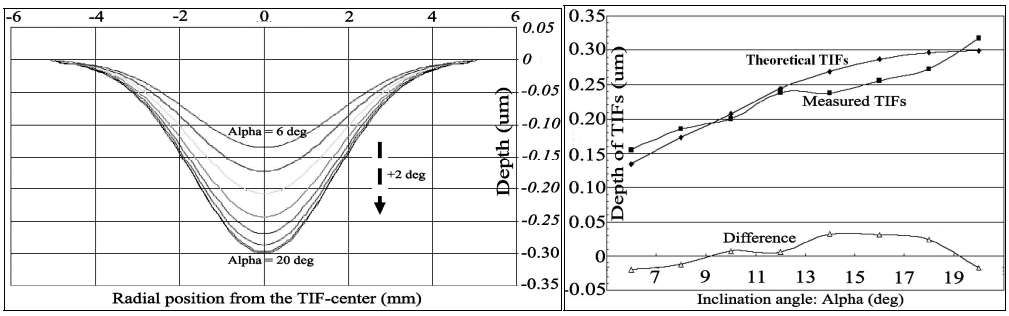

(a) (b)

Fig. 4. (a) Cross-sectional profiles of sTIFs (α: 6 - 20 degrees) and (b) depth of measured [13] and theoretical sTIFs

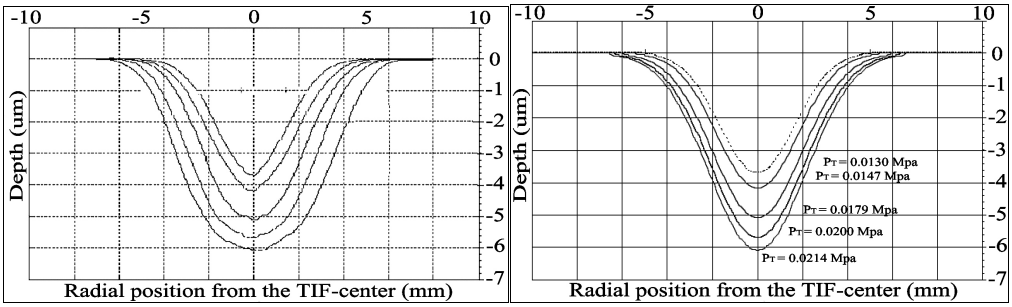

(a) (b)

Fig. 5. (a) Measured sTIFs [14] and (b) theoretical sTIFs (P_T: 0.0130 - 0.0214 Mpa)

3. Reverse computation of actual polishing pressure from TIF

The precessing tool bonnet is a complex mechanical system of pressurized membrane, cement, and polishing cloth. Therefore, an accurate, mechanical model of the bonnet system is not easily obtainable from straightforward integration of its mechanical element characteristics. A simpler way of characterizing and, hence, optimizing the bonnet system, is to establish a computational process to derive the actual polishing pressure distribution for a set of chosen tooling parameters, from combination of the empirical TIFs and theoretical model.

The first step of the computation process for the actual polishing pressure $P_{E(i)}$ starts with Eq. (6) which is a re-arranged form of Eq. (5). $P_{E(i)}$ was calculated for 41 data points (N=41, $0 \le i \le 40$) at the interval of $\Delta\lambda$=0.5mm along the TIF cross-sectional profile of 20mm in diameter. This is the actual polishing pressure that the bonnet system exerts inside the polishing spot.

$$P_{E(i)} = \frac{\Delta z_{(i)}}{\kappa[(V_{TRx(i)} + V_{TFx})^2 + (V_{TRy(i)} + V_{TFy})^2]^{1/2} \Delta t} \tag{6}$$

The exact tooling parameters of the measured TIF [14] were not known, but since the shape proximity of both experimental and theoretical TIFs are well demonstrated in Fig. 5, the five theoretical TIFs in Fig. 5(b) were used as input Δz data instead. The resulting (computed) pressure profiles are depicted in Fig 6(a). Here we re-confirm the aforementioned expectation that, after the removal of tool speed and dwell time effects, the real polishing pressure exerted by the bonnet has edgeless near Gaussian shapes. This implies that the Gaussian pressure

#6258 - $15.00 US Received 10 January 2005; revised 27 January 2005; accepted 27 January 2005

distribution inside the polishing spot is a valid approximation for any empirical TIFs of near Gaussian shapes in precessing tool polishing.

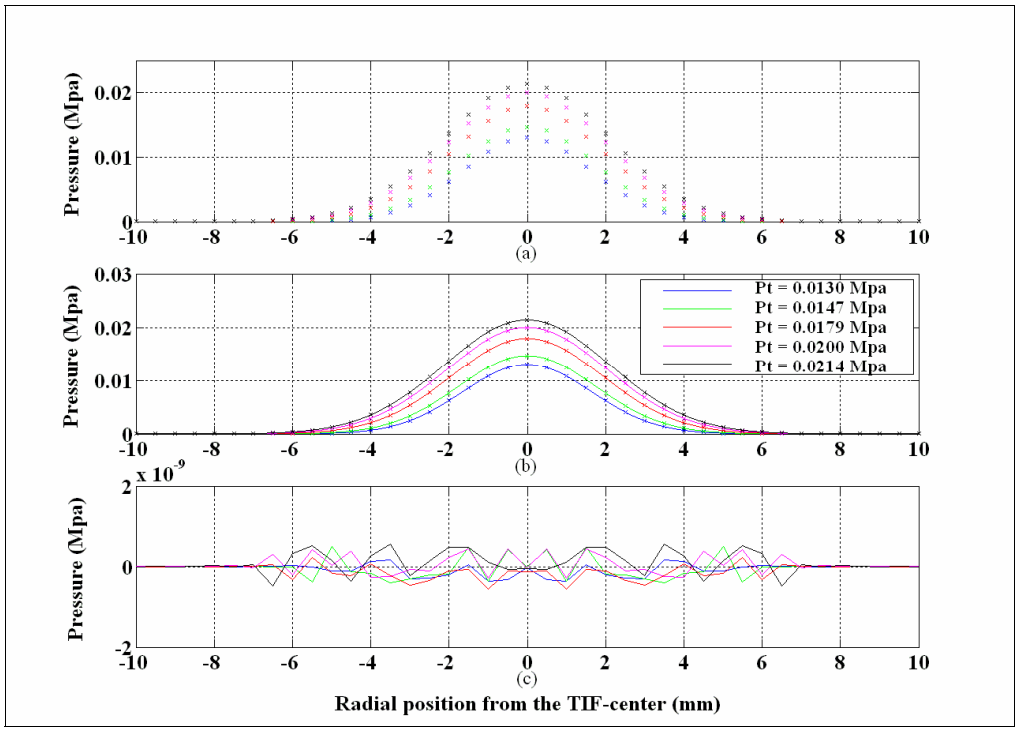

Fig. 6. (a) Empirical polishing pressure data (41 data points) inverse-computed from TIFs, (b) theoretical polishing pressure expressed with modified Gaussian function fitted to the data and (c) residual pressure difference between the data and the fitted functions

The second step is to fit the modified Gaussian function of Eq. (3) to the empirical polishing pressure distributions, $P_{E(i)}$, in Fig. 6(a). For each computation data point of $0 \le i \le 40$, the pressure difference $d_{(i)}$ between $P_{E(i)}$ (computed from TIF in Fig. 5(b)) and $P_{(i)}$ (theoretical polishing pressure model as in Eq. (3)), is expressed as Eq. (7). We then defined the standard deviation of the pressure differences σ_d as Eq. (8). The simplex search method [19] was used for the function fitting algorithm, which searches for the optimum parameter set (P_T, σ, and ψ) until it reaches the minimum standard deviation σ_d.

$$d_{(i)}(P_T, \sigma, \psi) = (P_{E(i)} - P_{(i)}) \tag{7}$$

$$\sigma_d(P_T, \sigma, \psi) = [\frac{1}{N}\sum_{i=1}^{N}(d_{(i)} - \bar{d})^2]^{1/2} = \{\frac{1}{N}\sum_{i=1}^{N}[d_{(i)} - (\frac{1}{N}\sum_{i=1}^{N} d_{(i)})]^2\}^{1/2} \tag{8}$$

Table 2 lists the optimum parameter sets for the resulting Gaussian functions shown in Fig. 6(b) and the fitting accuracy in terms of the standard deviation σ_d, which represents the pressure difference plotted in Fig. 6(c). Both Table 2 and Fig. 6(c) show the extreme accuracy of the function fit, since the standard deviation of the pressure differences σ_d is on the order of e-10 Mpa. This shows that this theoretical model can be successfully used to optimize the bonnet system, by unlocking the relationship between TIF, pressure and velocity in precessing tool polishing. It is worth noting that if the TIF shapes depart significantly from the modified Gaussian function used in this study, the accuracy of the function fit may be degraded.

#6258 - $15.00 US Received 10 January 2005; revised 27 January 2005; accepted 27 January 2005

Table 2. Optimized parameters (P_T, σ, and ψ) and standard deviation σ_d for the modified Gaussian function fitting

Maximum depth of input TIF (Fig. 5(b))	Peak polishing pressure (reverse calculated)	Modified Gaussian function parameters after optimized fitting			Standard deviation representing minimum fitting errors
(um)	*(Mpa)*	P_T	σ	ψ	σ_d
		(Mpa)	*(mm)*	*dimensionless*	*(Mpa)*
3.704	0.0130	0.0130	18.356	124.5128	1.8165e-10
4.185	0.0147	0.0147	19.3907	122.9192	2.3265e-10
5.090	0.0179	0.0179	19.4704	101.8420	2.1121e-10
5.682	0.0200	0.0200	17.4415	73.1725	2.2649e-10
6.077	0.0214	0.0214	19.2835	83.6167	2.4838e-10

4. Concluding remarks

As the first of two studies in series, the theoretical basis for a new three dimensional polishing simulation technique is reported for efficient fabrication of 2m class hexagonal segment mirrors for ELT projects. The theoretical static tool influence function (sTIF) of the bulged precessing tooling was established, and its applicability for polishing simulation was verified by comparing the computer generated (theoretical) sTIFs against the measured TIFs [13,14] for various polishing parameters. We then report a reverse computation technique to obtain the actual polishing pressure from the combination of measured TIF and the theoretical model. The results are useful for optimizing the bonnet system by unlocking the relationship between TIF, pressure and velocity in precessing tool polishing. Using the theoretical TIF studied here, a new fabrication simulation technique for 2m class hexagonal segmented mirrors for the EURO50 telescope project will be reported in the second study [17] in the series.

Acknowledgments

We acknowledge the financial support under the KISTEP Grant 2004-02622. We thank Tom Zobrist who guarded us against a number of unclarities in the final manuscript preparation.

#6258 - $15.00 US Received 10 January 2005; revised 27 January 2005; accepted 27 January 2005